Catal Lett (2009) 128:356–362
DOI 10.1007/s10562-008-9753-5

Partial Oxidation of Isobutane over Vanadium Phosphorus Oxides

Jingqi Guan · Zhuqian Wang · Chen Xu · Ying Yang · Bo Liu · Xiaofang Yu · Qiubin Kan

Received: 8 September 2008 / Accepted: 23 October 2008 / Published online: 11 November 2008

Abstract A series of vanadium phosphorus oxides (VPO) were prepared by using dodecyl amine as surfactant and tested for the partial oxidation of isobutane and isobutene. Characterization results showed that their structure and properties depend on the content of dodecyl amine. Catalytic tests showed that relatively high isobutane conversion and desired product selectivity can be achieved over a proper dodecyl amine doping VPO catalyst. It is also found that higher isobutane conversion can be achieved over V^{4+}-containing phases as compared to V^{5+}-containing phases, while proper surface V^{5+}/V^{4+} ratio may be propitious to obtain high selectivity to methacrylic acid for the selective oxidation of isobutane. In addition, the content of dodecyl amine in the preparation of the VPO catalysts appears to be more important in determining the surface P/V ratio of the catalysts.

Keywords Isobutane · Isobutene · Vanadium phosphorus oxide · Selective oxidation · Methacrylic acid

1 Introduction

It is well known that partial oxidation of *n*-butane to maleic anhydride (MA) is the only commercialized process for light paraffin conversion [1, 2]. The key factor of the success is that the designed product MA is very stable for further oxidation due to its strong C–H bond energy. However, after a lot of efforts developing catalysts for many years, the selective oxidation of isobutane to methacrolein (MAL) and methacrylic acid (MAA) is still classified as a highly difficult reaction. The reason for this problem is the reactive methyl group of produced MAL and MAA, which are highly unstable against further oxidation to generate complete oxidation products. Generally, in order to obtain high selectivity to MAL and MAA, oxygen insertion to the double bond of the isobutene intermediate should be much faster than oxidation C–H bond fission at the methyl group. Therefore, catalysts possessing multi-functional properties should be designed for the selective oxidation of isobutane.

V-based catalysts have been the object of numerous investigations, because they correspond to a general composition used in the great majority of catalysts active for obtaining isobutene from isobutane [3]. However, vanadium phosphorus oxide (VPO) has seldom been studied in the selective oxidation of isobutane [4], although VPO is well known as effective catalyst for the selective oxidation of *n*-butane to MA [1, 2]. It is generally accepted that well crystallized $(VO)_2P_2O_7$ is the major phase that is present in an industrial VPO catalyst, whereas the participation of V^{5+} species in the form of $VOPO_4$ phases, disperses on the surface V^{4+}/V^{5+} couples or surface and bulk crystalline defects in the catalytic process [5, 6]. However, the exact stoichiometry and structure of the active and selective component(s) in the mixture of phases and variants of structures it contains is still the object of a debate. It is therefore attractive to investigate the catalytic performance of alkane oxidation over VPO system catalysts.

J. Guan · Z. Wang · C. Xu · Y. Yang · B. Liu · X. Yu · Q. Kan (✉)
College of Chemistry, Jilin University, Changchun 130023, People's Republic of China
e-mail: qkan@mail.jlu.edu.cn; catalysischina@yahoo.com.cn

Q. Kan
Jiefang road 2519, Changchun 130021, People's Republic of China

In the past years, there have been many reports about the synthesis of mesostructured vanadium phosphate (VPO) phases by using cationic (alkyl trimethyl ammonium salts), anionic (alkyl sulfonates and phosphates) and primary alkylamines as structure directing surfactants [7–17]. However, these materials are mainly applied in relatively low temperature reaction because the surfactant is inevitably lost at relatively high temperature. Therefore, it is necessary that these samples should be calcined at a high temperature to eliminate the surfactant for the catalytic oxidation of alkanes.

In this paper, we present how the incorporation of dodecyl amine to a VPO catalyst has a promoter effect on the catalytic performance for the selective oxidation of isobutane. In addition, we reported the major crystalline phases found in the VPO oxide catalysts which were characterized by XRD. Moreover, the oxidation state of surface V atoms was also investigated by XPS.

2 Experimental

2.1 Catalyst Preparation

The following chemicals were commercially available and used as received: dodecyl amine (>99%, Tianjin Fine Chemical Company), V_2O_5 (>99%, Beijing Fine Chemical Company), H_3PO_4 (85%, Beijing Fine Chemical Company).

Dodecyl amine (**DA**) was intercalated into $VOHPO_4 \cdot 0.5H_2O$ by an organic solvent method [7]. In a typical synthesis, 1.82 g (0.01 mol) of V_2O_5 was suspended in a mixture of 20 mL of isobutyl alcohol and 10 mL of benzyl alcohol. The suspension was stirred under reflux at 120 °C for 8 h and then cooled to room temperature. Different amounts of **DA** (N/V molar ratio = 0, 1:2, 1:1, 3:2, and 2:1) were added to the solution, which was boiled for 30 min to get a homogeneous dispersion. Afterward, 2.30 g (0.02 mol) of 85% H_3PO_4 in 10 mL of benzyl alcohol was dropped into the suspension in 2 h. The mixture was further treated under reflux (120 °C) for 10 h. After the suspension was cooled to room temperature, the resultant slurry was filtered, washed with isobutanol for several times, then dried at room temperature for 12 h to obtain the catalyst precursor (coded as P-NV0, P-NV12, P-NV11, P-NV32, and P-NV21, according to N/V molar ratio), which was calcined under a flow of air (100 mL/min) at 500 °C (raising temperature rate of 2 °C/min) for 8 h to obtain the corresponding catalyst (denoted as C-NV0, C-NV12, C-NV11, C-NV32, and C-NV21).

2.2 Catalyst Characterization

Specific surface areas of the catalysts were measured based on the adsorption isotherms of N_2 at −196 °C using the BET method (Micromeritics ASAP2010). Powder X-ray diffraction (XRD) patterns were collected using a Shimadzu XRD-6000 scanning at 4°/min with CuK_α radiation (40 kV, 30 mA). Infrared spectra (IR) of the samples were recorded at room temperature using a NICOLET Impact 410 spectrometer.

X-ray photoelectron spectra (XPS) were recorded on a VG ESCA LAB MK-II X-ray electron spectrometer using AlK_α radiation (1486.6 eV, 10.1 kV). The spectra were referenced with respect to the C_{1s} peak at 284.7 eV. Measurement error of the spectra was ±0.2 eV.

H_2-temperature programmed reduction (TPR) experiments were carried out in a flow reactor system, in which 10 mg of catalyst was charged each run into a U-shaped quartz microreactor (4 mm i.d.). After purging with Ar gas from 50 to 300 °C at a ramp rate of 10 °C/min, holding at 300 °C for 30 min, and cooling to 100 °C, the sample was reduced in a 5% H_2/Ar stream (25 mL/min). The reduction temperature was raised uniformly from 100 to 800 °C at a ramp rate of 10 °C/min. H_2 consumption was measured by a thermal conductivity detector (TCD).

2.3 Catalytic Tests

The reaction was performed in a stainless steel tubular fixed bed reactor (16 mm i.d., 400 mm long) under atmospheric pressure. Each catalytic test was carried out using 1.0 g of catalyst, which was granulated into particles of 20–30 mesh size and diluted with 1.0 g of SiC particles to prevent temperature gradients and hot spots in the reactor. Under our reaction conditions, the homogeneous reaction can be neglected. Carbon mass balances of ≥97% were typically observed.

Reaction feed was controlled by a mass flow controller, and water was fed by a mini-pump. The catalytic reaction condition was as follows: molar ratio of the feed gas $i\text{-}C_4H_{10}:O_2:N_2:H_2O = 1:2:2:2$, $i\text{-}C_4H_8:O_2:N_2:H_2O = 1:2:5:2$. The products were then fed via heated lines to an on-line gas chromatography for analysis. Methacrolein (MAL), methacrylic acid (MAA), CO_x (CO, CO_2), and acetic acid (HAC) were the main products. Small amounts of propylene ($C_3^=$), isobutene ($i\text{-}C_4^=$), acetone, acrolein, and acrylic acid were also detected.

3 Results and Discussion

3.1 XRD Studies

The XRD patterns of mesostructured VPO synthesized using different content of **DA** surfactant are shown in Fig. 1. It is obvious that the product NV0 synthesized from a mixture of reactants without **DA** shows no diffraction peak in the 2θ

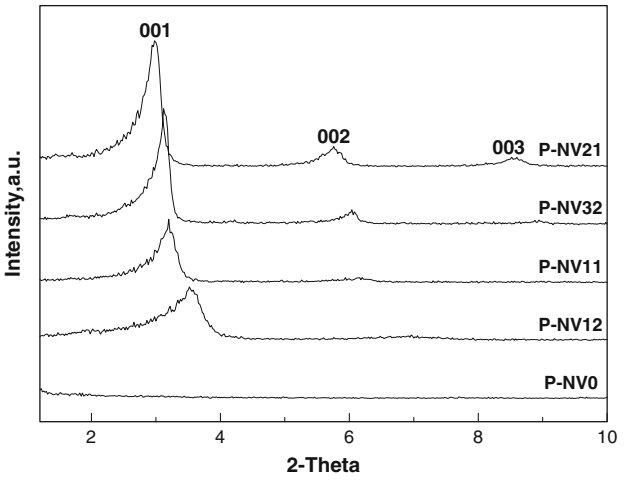

Fig. 1 XRD patterns of as-synthesized mesostructured VPO phases prepared using different content of **DA** surfactant

region of 1.2–10.0° in the XRD pattern, but yields many peaks at 10–40° (not shown here). However, VPO catalyst prepared by using **DA** (e.g., N/V = 1/2) shows two reflections at 3.5° and 6.9° corresponding to the (0 0 1) and (0 0 2) reflections, indicating that a lamellar VPO mesophase is obtained [7, 10, 16]. Therefore, it is apparent that the existence of **DA** is essential to the formation of VPO having the mesoporous structure. Furthermore, the low angle peaks in XRD pattern are found to shift toward lower 2θ angles with increasing the content of **DA**, implying the formation of larger mesopores. In the meanwhile, the intensity of the diffraction peak corresponding to the (0 0 1) reflection became stronger with increasing the N/V molar ratio suggesting the improvement of crystallinity of **VPO-DA**.

The XRD patterns of the prepared catalysts calcined at 500 °C in air are depicted in Fig. 2. In the case of the sample C-NV0, the peaks at $2\theta = 10.7°$, 14.9°, 21.5°, 29.2°, 30.0°, 35.7°, 42.3°, 45.6°, and 46.7° can be assigned to $(VO)_3P_4O_{13}$ [50-0418], while the peaks at $2\theta = 18.1°$, 21.5°, 23.2°, 29.2°, 32.2°, 45.6°, and 46.7° can be attributed to γ-$VOPO_4$ [47-0950]. In the meanwhile, the XRD patterns of **DA**-synthesized VPO catalysts (C-NV12, C-NV32, and C-NV21) show that they also contain a mixed phase of $(VO)_3P_4O_{13}$ and γ-$VOPO_4$. However, it is worthy to mention that the C-NV11 catalyst has $(VO)_3P_4O_{13}$ phase as well as β-$VOPO_4$ phase, which is different from other **DA**-synthesized VPO catalysts. In addition, infrared measurement (not shown here) indicates that no C–H and C–O bands can be observed for **DA**-synthesized VPO catalysts, suggesting that the residual **DA** is entirely removed and the activated catalysts are **DA**-free after calcination.

The XRD patterns of the catalysts after reaction with isobutane are illustrated in Fig. 3. It is well known that products of the reaction likes oxygenates, water, and CO_x can interact with the catalytic material which should consequently change the surface and the bulk composition and thus change the distribution of the generated products all along the period of activation. As shown in Fig. 3, it is exhibited that $(VO)_3P_4O_{13}$ phase becomes the main phase for the five given VPO catalysts after reaction with isobutane, although γ-$VOPO_4$ phase is also detected. Compared to the C-NV0 catalyst before reaction, it is revealed that $(VO)_3P_4O_{13}$ phase becomes weaker, and amorphous phases are found after isobutane reaction. It is also of interest to notice that only $(VO)_3P_4O_{13}$ and γ-$VOPO_4$ phases exist, while β-$VOPO_4$ phase is not detected in the C-NV11 catalyst after reaction, demonstrating that electron and oxygen species are carried between the surface and the bulk of the oxide. In other words, the surface of the VPO catalyst was slowly reduced with the time of reaction, which leads to the transformation of the phases in the bulk (e.g., β-$VOPO_4$ to $(VO)_3P_4O_{13}$ and γ-$VOPO_4$).

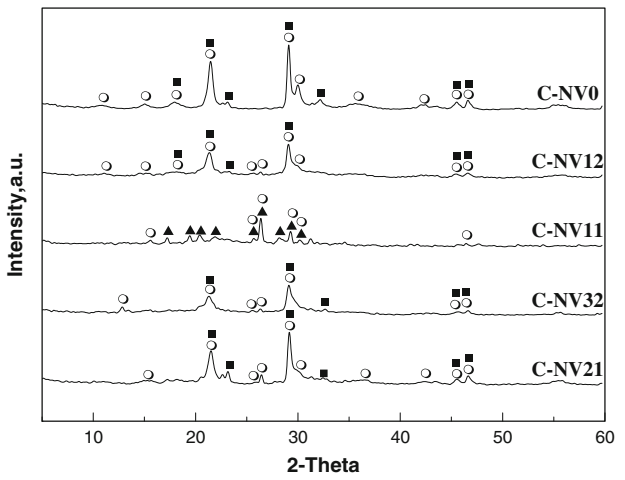

Fig. 2 XRD patterns of samples calcined at 500 °C in air: (■) γ-$VOPO_4$; (▲) β-$VOPO_4$; (○) $(VO)_3P_4O_{13}$

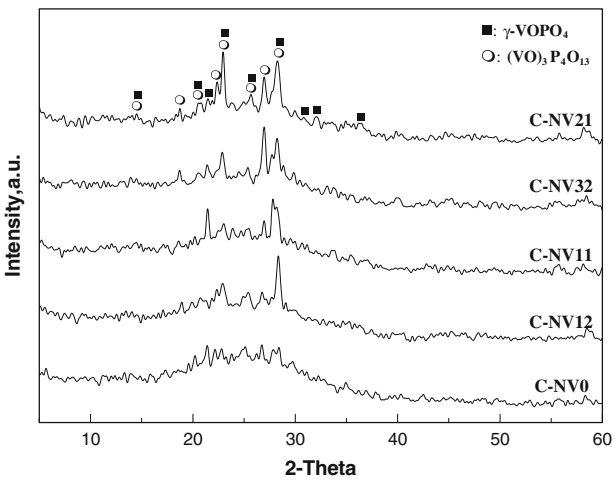

Fig. 3 XRD patterns of VPO catalysts after reaction with isobutane

3.2 XPS Studies

To gain deeper insight into the surface constitution and properties of these catalysts, their V2$p_{3/2}$ binding energies are investigated and corresponding spectra are displayed in Fig. 4, which are composed and integrated with the results shown in Table 1. The V 2$p_{3/2}$ peak of catalysts could be fitted into two components at 516.9 and 518.0 eV, which can be related to V^{4+} and V^{5+} species, respectively [18–20]. Thus, the surface V^{5+}/V^{4+} atomic ratio is found to increase in the sequence C-NV11 < C-NV12 < C-NV32 < C-NV0 < C-NV21. This result shows that the surface V^{5+}/V^{4+} distribution could be modified by doping **DA** into VPO system. This information is remarkably important for catalytic considerations: the chemical reaction implies generally the interaction of the organic reagent and dioxygen at the surface of the oxides. As shown in Fig. 4 and Table 1, it is evident that the surface V^{5+}/V^{4+} atomic ratios of the used catalysts (R-NV0 and R-NV11) are much lower than those of the corresponding fresh catalysts suggesting that a part of V^{5+} in the fresh catalysts are reduced to V^{4+} after reaction.

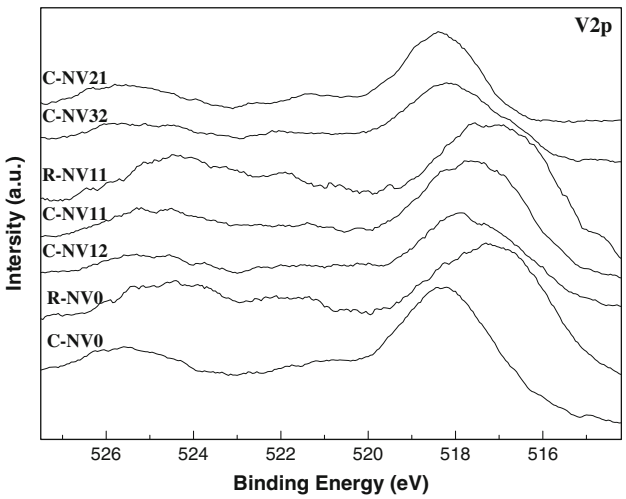

Fig. 4 X-Ray photoelectron spectra corresponding to the main transitions (V 2$p_{3/2}$) of the calcined catalysts before and after reaction with isobutane

As shown in Table 1, the P2p binding energies of surface phosphorus are very similar (ca. 133.2 eV) for all of the samples. It is revealed that the element of P is enriched on the surface, which is a common phenomenon for VPO catalysts [21]. It is generally accepted that a slight excess of phosphorus somehow helps stabilize the V^{4+} oxidation state and limits the over oxidation of a V^{4+}-containing phase to a V^{5+} phosphate both in the reactant's atmosphere and in air. However, the suggestion does not consist with our observation. As can be seen from Table 1, there are much higher surface P/V ratios on the C-NV32 and C-NV21 catalysts than those on the other catalysts, while the surface V^{4+}/V^{5+} atomic ratios of the two catalysts are remarkably lower than the other catalysts. In addition, the high surface P/V ratio indicates that the surface of working VPO catalysts consists of an amorphous layer, probably not detectable by XRD. This observation can be confirmed by the XRD patterns of the used catalysts with similar high surface P/V ratio (shown in Table 1). It is clear that there are amorphous phases in the R-NV0 and R-NV11 catalysts and their surface P/V ratios increase compared with the fresh catalysts indicating that a high P-containing phase is present in the amorphous layer. Martin et al. [22] also reported a similar phenomenon in a study on solid state reaction of $(NH_4)_2VOP_2O_7$ in the presence of ammonia.

3.3 H_2-TPR Studies

For the selective oxidation of isobutane over VPO catalyst, redox cycle of vanadium generally involves reduction of V^{5+} and V^{4+}, and the further reduction of V^{3+} is negligible in this system. According to previous reports [23–26], reduction of V^{5+} and V^{4+} is usually taken place in the temperature range of 25–800 °C. In Fig. 5, the TPR profiles of the calcined catalysts are plotted. Generally, the peaks

Table 1 XPS data of the calcined catalysts before and after reaction with isobutane

Sample	Binding energy (eV)			Surface composition (at %)				Surface oxidation states	Average oxidation number
	V2$p_{3/2}$	P2p	O1 s	V	P	O	P/V	V^{5+}/V^{4+}	V^{n+}
C-NV0	518.2	133.0	531.1	9.3	12.6	78.1	1.4	0.78/0.22	4.78
R-NV0[a]	517.1	133.9	531.2	8.5	20.7	70.8	2.4	0.48/0.52	4.48
C-NV12	517.7	133.2	531.1	8.3	13.6	78.1	1.6	0.69/0.31	4.69
C-NV11	517.6	133.3	531.4	9.7	11.4	78.9	1.2	0.55/0.45	4.55
R-NV11[a]	517.1	134.0	531.4	8.3	21.6	70.1	2.6	0.27/0.73	4.27
C-NV32	518.1	133.2	531.4	7.1	19.1	73.8	2.7	0.94/0.06	4.94
C-NV21	518.3	133.3	531.2	6.9	21.4	71.7	3.1	0.99/0.01	4.99

[a] After reaction with isobutane

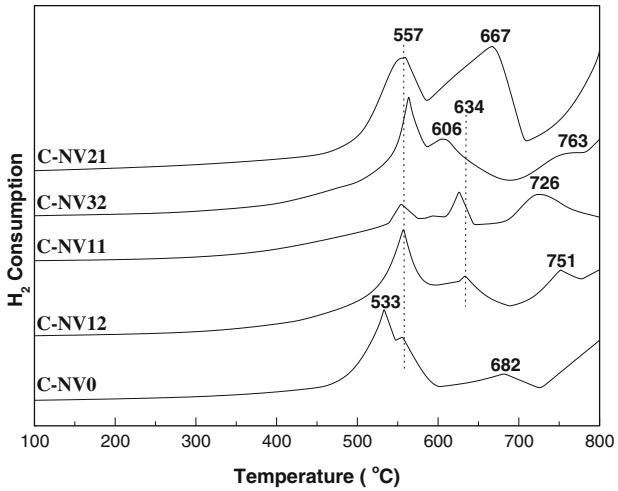

Fig. 5 The H_2-TPR profiles of samples calcined at 500 °C in air

present in the ca. 500–700 °C range are attributed to the removal of oxygen related to V^{5+} species, while the TPR profile shows a main peak in the ca. 700–800 °C range, attributable to the removal of lattice oxygen related to V^{4+} species [26–29]. Compared with the first reduction peak of the **DA**-synthesized VPO, the first reduction peak of the C-NV0 sample occurs at lower temperature (533 °C), suggesting that the lattice oxygen is more reactive.

In order to estimate the H_2 consumption, the area of TPR profile is integrated (Table 2). The results of Table 2 indicate that the total H_2 consumption (μmol/10 $mg_{cat.}$) is 20.3 for C-NV0, 56.6 for C-NV12, 55.2 for C-NV11, 55.5 for C-NV32, and 64.7 for C-NV21. Consequently, the total H_2 consumption increases in the sequence C-NV0 < C-NV11 ≈ C-NV32 < C-NV12 < C-NV21. However, the H_2 consumption of the catalysts corresponding to low temperature (about 560 °C) increases with increasing the content of **DA** in the synthesized process and reaches a maximum when the N/V molar ratio is 3/2. In addition, it is apparent that for C-NV12, C-NV11 and C-NV32, a large H_2 consumption can be seen at high temperature region (700–800 °C). Such behavior seems to be related to changes in the nature of the crystalline phases by a **DA**-synthesized route. Namely, the reducibility of the VPO catalyst is improved by **DA** treatment.

3.4 Catalytic Properties

BET specific surface areas and catalytic behaviors of the five catalysts prepared for this study are presented in Table 3. The sample C-NV0 without addition of **DA** in the synthesized route possesses the largest specific surface area, while the specific surface area of the samples synthesized with **DA** obviously decreases. For instance, it is only 5.6 m^2/g^{-1} as the N/V molar ratio is 1/2 in the synthesized gel. However, the specific surface area may slightly increase with further augmenting the N/V molar ratio up to 2/1 in the preparation of catalyst precursor.

The effects of **DA** surfactant content on the possible active phases and catalytic behavior of VPO catalysts were evaluated, and the results are summarized in Table 3. It can be seen that the conversion of isobutane decreases with initial addition of **DA** surfactant, but it gradually increases with the further increase of **DA** surfactant. The change of isobutane conversion would be explained by the corresponding change of the specific surface areas of the tested

Table 2 The H_2-TPR results of samples calcined at 500 °C in air

	Sample				
	C-NV0	C-NV12	C-NV11	C-NV32	C-NV21
Temperature (°C)	533/565/682	557/634/751	557/627/726	563/606/763	557/667
Weight (mg)	10	10	10	10	10
H_2 consumption (μmol)	14.4/3.5/2.4	18.8/9.9/27.9	21.9/3.5/29.8	26.8/8.1/20.6	24.3/40.4

Table 3 Catalytic data of the catalysts for isobutane oxidation at 380 °C[a]

Sample	S_{BET} (m^2/g^{-1})	Conversion (%)	Selectivity (%)							
			i-$C_4^=$	MAL	MAA	CO	CO_2	$C_3^=$	ACT	HAC
C-NV0	13.3	20.4	0	3	11	45	20	4	0	17
C-NV12	5.6	17.3	5	17	16	29	10	8	2	13
C-NV11	5.7	17.5	2	18	26	29	10	6	3	6
C-NV32	5.7	17.6	5	20	16	29	10	8	4	8
C-NV21	8.3	18.3	0	5	14	43	15	6	0	17

[a] Reaction condition: i-C_4H_{10}:O_2:N_2:H_2O = 1:2:2:2 (mol), GHSV = 3000 ml h^{-1} g_{cat}^{-1}

catalysts, whereas the astonishing variety of the MAL and MAA selectivity would not follow the trend. As can be found from Table 3, the selectivity to MAL and MAA is considerably improved by the addition of small amount of **DA** surfactant. For example, the selectivity to MAL and MAA reaches 17% and 16%, respectively, as the N/V ratio is as low as 1/2. The selectivity to MAL and MAA increases continuously with the increase of **DA-**content, and reaches 20% for MAL selectivity and 26% for MAA selectivity when the N/V ratio increases up to 3/2 and 1/1, respectively. However, their selectivities decrease with further increasing content of **DA** surfactant. Therefore, it can be concluded that the addition of **DA** has a positive effect on the formation of MAL and MAA for the selective oxidation of isobutane over VPO catalyst.

Combined with the XRD results of VPO catalysts after reaction with isobutane, it is confirmed that V^{4+}-containing $(VO)_3P_4O_{13}$ is the dominant phase in the reacted catalysts. It is therefore rational to suppose that V^{4+}-containing phase (e.g., $(VO)_3P_4O_{13}$) may play an important role in the formation of MAL and MAA. The results on catalytic performances with time-on-stream show that the isobutane conversion is doubled after a period of first 7 h reaction compared to the initial activity, whereas a steep decrease (about 16%) in MAA selectivity is observed at the same time (not shown here). Afterwards, the catalytic performance is almost steady. In view of the higher surface V^{5+} content before reaction than after reaction, it is therefore assumed that the VPO catalysts containing discrete amounts of V^{5+} sites have in general a better catalytic performance in the oxidation of isobutane than the catalysts which exclusively contain V^{4+} sites in good agreement with many reports for ethane oxidation, and *n*-butane oxidation [30–33]. It has been reported that the presence of a relatively high fraction of surface V^{4+} oxide species leads to a significant improvement of the catalytic performances in the oxidative dehydrogenation of ethane over a $VOPO_4/TiO_2$ catalyst. In addition, the selective oxidation of H_2S to sulfur proceeds only when V_2O_5 is substantially reduced (more than 20%), and then a redox mechanism on V_2O_5 catalysts is suggested [34–36].

According to our previous experiment, we found that the catalytic behavior of isobutane partial oxidation over V^{4+}-containing $(VO)_2P_2O_7$ catalyst is very bad. It is also inferred that the changes in the catalytic performance for selective isobutane oxidation to MAL and MAA mainly result from the variation of the bulk and surface V^{5+}/V^{4+} ratios [37]. However, the effect is very complex and the perfect V^{5+}/V^{4+} balance to achieve the best performance in selective oxidation of light alkanes is still not clear. We find that the reproducibility of the catalysts and the catalytic results is provided. In addition, the catalyst deactivation is under investigation.

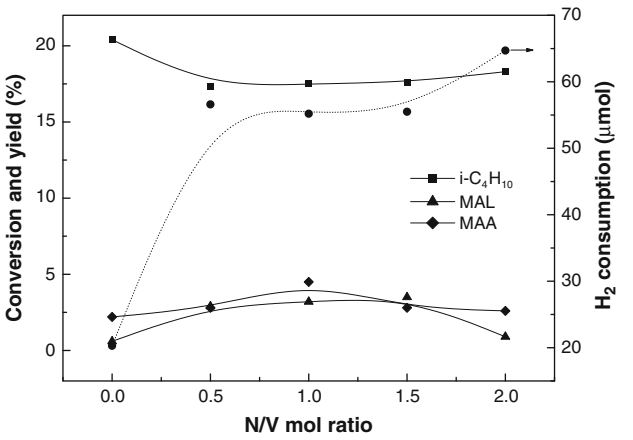

Fig. 6 Relationship of the H_2 consumption with the catalytic performance

In the meanwhile, the redox properties of the VPO catalysts also affect the catalytic performance of the catalysts in isobutane oxidation (shown in Fig. 6). A clear correlation is observed between the catalytic performance and physicochemical properties. Combined with the TPR results shown in Fig. 5, C-NV0 gives a slightly better reducibility compared to the **DA**-synthesized VPO and possesses higher labile and more reactive lattice oxygen at lower temperature which enhances the catalytic activity. However, a first increase in H_2 consumption is observed with increasing **DA**-content**,** and MAL and MAA yields increase, while isobutane conversion slightly decreases. But too high H_2 consumption for a catalyst is not favor the formation of MAL and MAA. The preferable MAL and MAA yield is achieved over C-NV32 and C-NV11 catalysts with appropriate H_2 consumption.

The reaction results of selective oxidation from isobutene to MAL and MAA over the catalysts at 380 °C given in Table 4 indicate that all of the VPO catalysts are less active and selective for the partial oxidation of isobutene to MAL as compared to bismuth molybdate system catalysts [38–40]. In opposition to the behavior of isobutane partial oxidation, C-NV0 catalyst achieves the best catalytic

Table 4 Catalytic data of the catalysts for isobutene oxidation at 380 °C[a]

Sample	Conversion (%)	Selectivity (%)						
		MAL	MAA	CO	CO_2	$C_3^=$	ACT	HAC
C-NV0	50.4	33	9	16	25	2	7	8
C-NV12	38.8	21	11	20	27	5	11	5
C-NV11	33.3	24	16	19	31	1	8	1
C-NV32	29.5	33	8	15	23	3	9	9
C-NV21	18.1	13	16	28	13	2	4	24

[a] Isobutene:O_2:N_2:H_2O = 1:2:5:2 (mol); GHSV = 1800 mL h^{-1} g_{cat}^{-1}

performance. In the meanwhile, it is apparent that relatively high MAL selectivity is obtained over C-NV32 catalyst. Considering that relatively high V^{5+}/V^{4+} ratios are detected on the surface of the two VPO catalysts, it can be concluded that the presence of appropriate V^{5+} ions on the surface of catalysts favors the formation of MAL. However, one can find that too high surface V^{5+} content (i.e., C-NV21 catalyst) may lower the selectivity to MAL due to its overoxidation.

In addition, it can be concluded that the selectivity to MAA in the selective oxidation of isobutane over VPO catalysts (Table 3) is generally higher than that in the selective oxidation of isobutene (Table 4). Therefore, it is reasonable to propose that MAA is formed not only from isobutene and MAL, but also directly from isobutane or an intermediate. In other words, MAA is formed following a parallel-consecutive scheme: the consecutive path of the reaction may include the steps: isobutane → isobutene → MAL → MAA → CO_x.

4 Conclusions

Activated vanadium phosphate catalysts were obtained by calcining **VPO-DA** precursors. BET surface area showed that **DA**-series catalysts gave lower surface area as compared to the sample prepared with no **DA**. Reduction profiles of VPO catalysts gave reduction peaks associated with V^{4+} and V^{5+} species, while the lattice oxygen in C-NV0 catalyst is more reactive than **DA**-series catalysts. Moreover, higher amount of H_2 consumption was related to **DA**-series catalysts. From the catalytic test for isobutane oxidation, **DA**-series catalysts show higher MAL and MAA selectivity compared with the **DA**-free catalyst. The V^{4+}-containing $(VO)_3P_4O_{13}$ phase is suggested to be active for isobutane oxidation, while the presence of small V^{5+} species may favor the formation of MAA. Under our reaction conditions, the C-NV11 catalyst achieved the best MAL and MAA selectivity (44%) and yield (7.7%) at 380 °C.

Acknowledgments We acknowledge the financial supports from the National Basic Research Program of China (2004CB217804) and the National Natural Science Foundation of China (20673046).

References

1. Hodnett BK (1985) Catal Rev-Sci Eng 27:373–424
2. Centi G, Trifiro F, Ebner JR, Franchetti VM (1988) Chem Rev 88:55–80
3. Takita Y, Hikazudani S, Soda K, Nagaoka K, Mol J (2008) Catal A Chem 280:164–172
4. Matsuura I, Aoki Y (1994) US Patent 5,329,043
5. Aït-Lachgar K, Abon M, Volta JC (1997) J Catal 171:383–390
6. Hutchings GJ, Kiely CJ, Sananes-Schulz MT, Burrows A, Volta JC (1998) Catal Today 40:273–286
7. Guliants VV, Benziger JS, Sundaresan S (1994) Chem Mater 6:353–356
8. Abe T, Taguchi A, Iwamoto M (1995) Chem Mater 7:1429–1430
9. Doi T Miyake T (1996) Chem. Commun: 1635–1636
10. Haskouri JE, Roca M, Cabrera S, Alamo J, Beltran-Porter A, Beltran-Porter D, Marco MD, Amoros P (1999) Chem Mater 11:1446–1454
11. Mizuno N, Hatayama H, Uchida S, Taguchi A (2001) Chem Mater 13:179–184
12. Schüth F (2001) Chem Mater 13:3184–3195
13. Carreon MA, Guliants VV (2002) Microporous Mesoporous Mater 55:297–304
14. Dasgupta S, Agarwal M, Datta A (2002) J Mater Chem 12:162–164
15. Carreon MA, Guliants VV, Guerrero-Pérez MO, Bañares MA (2004) Microporous Mesoporous Mater 71:57–63
16. Dasgupta S, Agarwal M, Datta A (2004) Microporous Mesoporous Mater 67:229–234
17. Datta A, Dasgupta S, Agarwal M, Ray SS (2005) Microporous Mesoporous Mater 83:114–124
18. Albonetti S, Cavani F, Trifiro F, Venturoli P, Calestani G, López Granados M, Fierro JL (1996) J Catal 160:52–64
19. Delishere P, Bere KE, Abon M (1998) Appl Catal A Gen 172:295–309
20. Guan JQ, Wu SJ, Wang HS, Jing SB, Wang GJ, Zhen KJ, Kan QB (2007) J Catal 251:354–362
21. Li X, Ji W, Zhao J, Zhang Z, Au C (2006) J Catal 238:232–241
22. Martin A, Steinike U, Rabe S, Lücke B, Hannour FK (1997) J Chem Soc, Faraday Trans 93:3855
23. Pierini BT, Lombardo EA (2005) Mater Chem Phys 92:197–204
24. Li X, Ji W, Zhao J, Zhang Z, Au C (2006) Appl Catal A Gen 306:8–16
25. Shen S, Zhou J, Zhang F, Zhou L, Li R (2002) Catal Today 74:37–43
26. Feng R, Yang X, Ji W, Chen Y, Au C (2007) J Catal 246:166–176
27. Wang X, Xu L, Chen X, Ji W, Yan Q, Chen Y, Mol J (2003) Catal A: Chem 206:261–268
28. Xiao C, Chen X, Wang Z, Ji W, Chen Y, Au C (2004) Catal Today 93–95:223–228
29. Taufiq-Yap YH, Saw CS (2008) Catal Today 131:285–291
30. Volta J-C, Acad CR (2000) Sci Paris, Serie IIc, Chemie 3:717–723
31. Han Y, Wang H, Cheng H, Deng J (1992) Chem Commun: 803–804
32. Casaletto MP, Lisi L, Mattogno G, Patrono P, Ruoppolo G (2004) Appl Catal A Gen 267:157–164
33. Ciambelli P, Galli P, Lisi L, Massucci MA, Patrono P, Pirone R, Ruoppolo G, Russo G (2000) Appl Catal A Gen 203:133–142
34. Centi G (1996) Appl Catal A 147:267–298
35. Shin MY, Nama CM, Park DW, Chung JS (2001) Appl Catal A Gen 211:213–225
36. Park DW, Park BK, Park DK, Woo HC (2002) Appl Catal A Gen 223:215–224
37. Guan J, Xu H, Jing S, Wu S, Ma Y, Shao Y, Kan Q Catal Commun (in press)
38. Oh-Kita M, Taniguchi Y (1991). European Patent 0,420,048A1, to Mitsubishi Rayon Co. Ltd
39. Watanabe S, Yoshioka H, Izumi J (1999) US Patent 5,856,259, to Mitsubishi Rayon Co. Ltd
40. Song N, Rhodes C, Bartley JK, Taylor SH, Chadwick D, Hutchings GJ (2005) J Catal 236:282–291